


Article

Optimization Study of Fluffy Materials Flocking Drainage Pipes to Resist Blockage Based on MD Binding Energy

Shiyang Liu ^{1,2,*} , Xuefu Zhang ^{1,2}, Yuanfu Zhou ^{1,2} and Feng Gao ^{1,2}

¹ State Key Laboratory of Mountain Bridge and Tunnel Engineering, Chongqing Jiaotong University, Chongqing 400074, China; zhangxuefu@cqjtu.edu.cn (X.Z.); 990201500027@cqjtu.edu.cn (Y.Z.); 990020701005@cqjtu.edu.cn (F.G.)

² College of Civil Engineering, Chongqing Jiaotong University, Chongqing 400074, China

* Correspondence: liushiyang@mails.cqjtu.edu.cn

Abstract: Drainage pipe blockage resulting from crystals is one of the causes for cracking and leakage of tunnel lining. Therefore, effective prevention from drainage pipe blockage caused by crystals is crucial to ensure the safety and stability of lining structures during the operation of tunnel drainage system. Based on a large number of indoor model tests and numerical simulation analyses, binding energy between four materials and the calcium carbonate aqueous solution (“solid + liquid” system) and that between the four materials and the two typical growth crystals of calcium carbonate (“solid + solid” system) were studied. The research results indicated that: (1) The four materials all had an adsorption effect on the calcium carbonate aqueous solution system, and the PA6 had the greatest adsorption effect while the PP had the smallest adsorption effect; (2) There was spontaneous adsorption between the PVC or PA6 and the two typical growth crystals of calcium carbonate and no adsorption between the PP or SiC and the two typical growth crystals of calcium carbonate unless external energy was in place; (3) The PP and SiC can be used as the materials for drainage pipe flocking, but it shall be ensured that the fluffy material has a good geometrical property. The prevention technology for crystallization that causes drainage pipe blockage fills the gap in the research of drainage pipe blockage caused by crystals, which can reduce the maintenance cost for the operation of the tunnel drainage system and ensure safe and normal operation of the tunnel.

Keywords: molecular dynamics; binding energy; crystallization prevention; flocking for resisting blockage; drainage pipe



Citation: Liu, S.; Zhang, X.; Zhou, Y.; Gao, F. Optimization Study of Fluffy Materials Flocking Drainage Pipes to Resist Blockage Based on MD Binding Energy. *Coatings* **2021**, *11*, 853. <https://doi.org/10.3390/coatings11070853>

Received: 25 June 2021

Accepted: 13 July 2021

Published: 15 July 2021

Publisher's Note: MDPI stays neutral with regard to jurisdictional claims in published maps and institutional affiliations.



Copyright: © 2021 by the authors. Licensee MDPI, Basel, Switzerland. This article is an open access article distributed under the terms and conditions of the Creative Commons Attribution (CC BY) license (<https://creativecommons.org/licenses/by/4.0/>).

1. Introduction

With the operation of tunnel projects, tunnel defects gradually emerge, among which drainage pipe blockage caused by crystals is a major factor affecting the service life of a tunnel. Carbonates formed by the inter-reaction of various ions of groundwater calcify into crystals over time, and these crystals accumulate in drainage pipes and cause blockage (Figure 1). Improper treatment of the crystals can affect the smooth operation of a tunnel drainage system and further lead to the cracking and leakage of the tunnel lining (Figure 2). Even worse, it may affect traffic safety and cause imponderable losses.

There are two kinds of causes for the blockage of tunnel drainage pipes. One is the environmental factor [1–3]: the concentration of ions such as calcium and magnesium in groundwater, the concentration of carbon dioxide in the air, and pH value of groundwater; the other is the construction factor [2,4]: concrete composition ratio, the form of the drainage system, etc. At present, research on the prevention technology of drainage pipe blockage caused by crystals is at the initial stage. The attachment of calcium carbonate crystals can be reduced through hydrophobic treatment on concrete base surfaces and PVC pipe walls with protective coating [5,6]; generation of crystals can be effectively lowered by optimizing the concrete materials and the concrete composition ratio, reducing the contact between groundwater and concrete, preventing CO₂ from entering the tunnel

drainage pipe, as well as adding appropriate fly ash to shotcrete [2,4]. Drainage pipe crystals mainly include insoluble calcite crystals, and the PEG-b-PAA-b-PS, poly(ethylene glycol)-block-poly(acrylic acid)-block-poly(styrene) can prevent the phase transition from vaterite to calcite [7]; in the presence of biopolymer, the relative content of vaterite increases with the application of ultrasonic treatment [8]; ultrasonic treatment makes the gathered calcium carbonate crystals more fragile [9]; RS1600, a green corrosion inhibitor, makes the crystal structure of calcium carbonate change from calcite to vaterite [10]; the cleaning solvent of organic acid reagents of single molecule carboxylic acids with a concentration of 2000 ppm and a dichromate index of 17.71% and that of polymerized carboxylic acids can effectively remove the karst crystal of a drainage pipe system while ensuring environmental protection [11]. Through a large number of 1:1 indoor model tests and numerical simulation analyses, Liu Shiyang, et al. [12–16] studied the feasibility and reliability of drainage pipe flocking for resisting blockage from a macro perspective, and some good flocking parameters were obtained. The real solution to the attachment of crystals of drainage pipes depends on the micro binding energy between the crystals and the drainage pipe. The presence of Fe^{2+} and Mg^{2+} can inhibit the growth of CaCO_3 , and the greater the concentration of Fe^{2+} or Mg^{2+} is, the stronger the inhibitory effect [17] will be. High voltage electric field can hinder the synthesis of calcium ions and carbonate ions and reduce the binding action of calcium ions or carbonate ions with the calcite growth crystal surface, and it also promotes the dissolution of scale [18].



Figure 1. Blockage of a tunnel drainage pipe caused by crystals.



Figure 2. Cracking and leakage of the tunnel lining.

From the above analysis, we can see that at present, many researches on the prevention technology of drainage pipe blockage caused by crystals are at a macro level, and there are few researches at a micro level. Therefore, based on the above indoor model tests and numerical simulation analyses, binding energy between the materials and crystals

was analyzed by the molecular dynamics software to find the best flocking materials for drainage pipes to resist blockage, which can provide a theoretical basis for the mechanism of resisting blockage by drainage pipe flocking.

2. Methods

2.1. Molecular Dynamics Software

Molecular Dynamics (MD) simulation has a history of about 50 years, whose success depends on the selection of an appropriate force field and a correct calculation method. The widely used MD simulation is becoming more and more important with the rapid development of computers. There are some commercial molecular dynamics computing software designed for the MD simulation, represented by the Materials Studio software of Accelry, which is a molecular dynamics simulation software featuring powerful functions, easy usage and clear images.

MD simulation considers the system to be studied as a collection of a large number of interacting particles whose motions follow the classical equation of motion (Newtonian equation, Hamiltonian equation or Lagrangian equation). By analyzing the force of each particle, equations of motion of various particles that constitute the system were numerically solved directly to obtain these particles' coordinates and momentum at every moment. Then, the microscopic state consisting of the coordinates and momentum was averaged against time to calculate the macroscopic properties such as multisystem pressures, energy and temperatures.

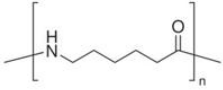
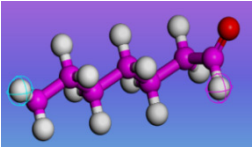
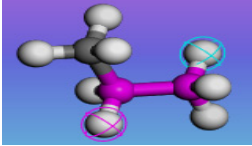
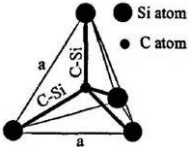
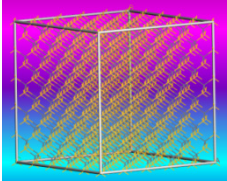
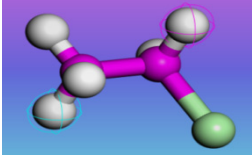
2.2. Model Building

From a micro level, different materials produce different binding energy with the groundwater solution system or the crystals' microscopic crystal surface. The stronger the binding energy is, the stronger the adsorption between the materials and the ions or the crystals' crystal surface in the solution will be. Thus, the anti-crystallization effect of fluffy materials was analyzed based on the intensity of binding energy. The characteristics of fluffy materials (Figure 3) and drainage pipe materials are shown in Table 1 below. The "solid–solid" model and the "solid–liquid" model were constructed with the amorphous cell of Materials Studio 8.0. The "solid–solid" model mainly included the double-layer model of different materials and the crystal surface of calcium carbonate crystals, and the "solid–liquid" model mainly included the double-layer model of different materials and calcium carbonate aqueous solution.

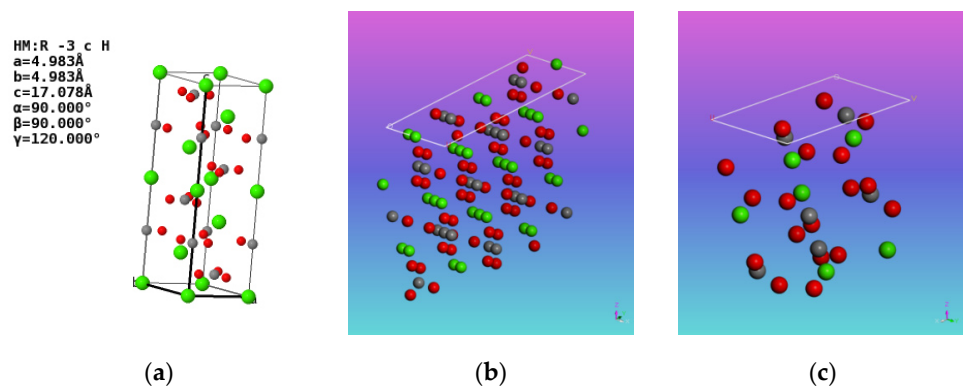


Figure 3. Three types of fluffy materials.

Table 1. The characteristics of fluffy materials and drainage pipe materials.

Material Category	Density	Chemical Composition	Chemical Formula	Structural Formula	Schematic Diagram
M1	1.13 g/cm ³	PA6	(C ₆ H ₁₁ NO) _n		
M2	0.90 g/cm ³	PP	(C ₃ H ₆) _n	$\left[\begin{array}{c} \text{CH}_3 \\ \\ \text{CH}-\text{CH}_2 \end{array} \right]_n$	
M3	3.20 g/cm ³	SiC	SiC		
PVC	1.38 g/cm ³	VCM	(C ₂ H ₃ Cl) _n	$\left[\begin{array}{c} \text{CH}_2-\text{CH} \\ \\ \text{Cl} \end{array} \right]_n$	

According to the Inorganic Crystal Structure Database (ICSD), calcite belongs to the R-3cH space group, with the spatial parameters of $a = b = 4.983 \text{ \AA}$, $c = 17.078 \text{ \AA}$, $\alpha = 90^\circ$, $\beta = 90^\circ$, $\gamma = 120^\circ$ (Figure 4). The study in [19] shows that the growth faces of calcite were (1 -1 0) and (1 0 4) crystal surfaces. The former was positively charged, while the latter was not charged. To obtain the binding energy between the materials and the calcite crystals, the models between different materials and the (1 -1 0) and (1 0 4) crystal surfaces were built respectively in the “solid–solid” model. The “solid–liquid” model mainly included the double-layer model of different materials and calcium carbonate aqueous solution. Given the low solubility of calcium carbonate, the calcium carbonate aqueous solution was formed with 350 water molecules, 3Ca^{2+} and 3CO_3^{2-} (Figure 5), and the solution volume was $21.74 \times 21.74 \times 19.34 \text{ \AA}^3$.

**Figure 4.** Details of the calcium carbonate calcite crystals: (a) calcite cell configuration; (b) (1 -1 0) crystal surface; (c) (1 0 4) crystal surface.

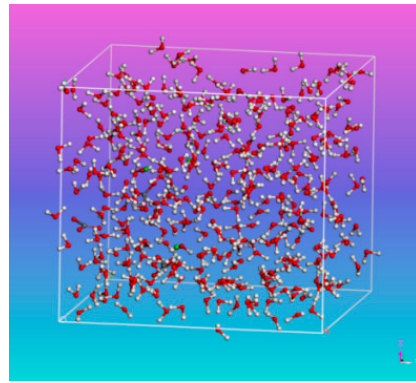


Figure 5. Calcium carbonate aqueous solution.

The supercell models of (1 $\bar{1}$ 0) and (1 0 4) crystal surfaces were built respectively through the command of Build \rightarrow Symmetry \rightarrow Supercell with a size of 21.74 Å \times 21.74 Å \times 17.60 Å; the polymer cells of the materials were built through the command of Modules \rightarrow Amorphous cell \rightarrow Calculation with a size of 21.74 Å \times 21.74 Å \times 19.34 Å. PVC is amorphous polymer, PA6, PP and SiC are crystalline polymer. PVC, PA6 and PP all construct amorphous polymer chain unit cells through single chain molecules, while SiC unit cells are obtained by expanding the unit cell structure of the software. First, geometric and energy optimization of all cells were performed. Then, the built upper and lower models were used to build the “solid + solid” model and the “solid + liquid” model through the command of Build \rightarrow Build layers in MS. The volume of the “solid + solid” model and that of the “solid + liquid” model were both 21.74 \times 21.74 \times 60 Å³, where the upper layer was calcium carbonate aqueous solution (supercells of (1 $\bar{1}$ 0) or (1 0 4) crystal surfaces) and the lower layer was polymer. A 5 Å vacuum layer is set between the upper and lower layers as the contact surface of the two materials, and a 20 Å vacuum layer is set at the top of the upper layer as the interface. The combination model of the materials and the supercells of (1 $\bar{1}$ 0) or (1 0 4) crystal surfaces is shown in Figures 6 and 7, and the combination model of the materials and the calcium carbonate aqueous solution is shown in Figure 8.

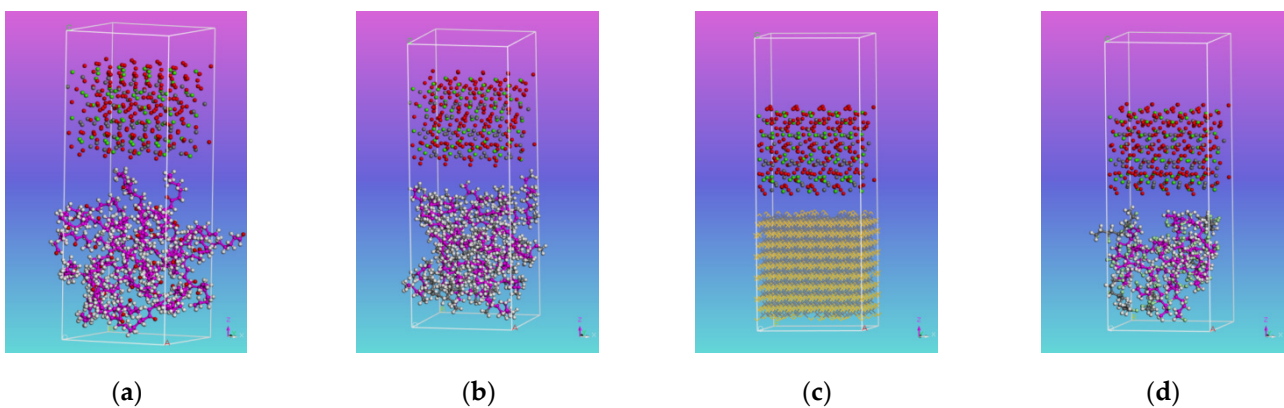


Figure 6. Combination model of the materials and the supercells of (1 $\bar{1}$ 0) crystal surface. (a) PA6-(1 $\bar{1}$ 0); (b) PP-(1 $\bar{1}$ 0); (c) SiC-(1 $\bar{1}$ 0); (d) PVC-(1 $\bar{1}$ 0).

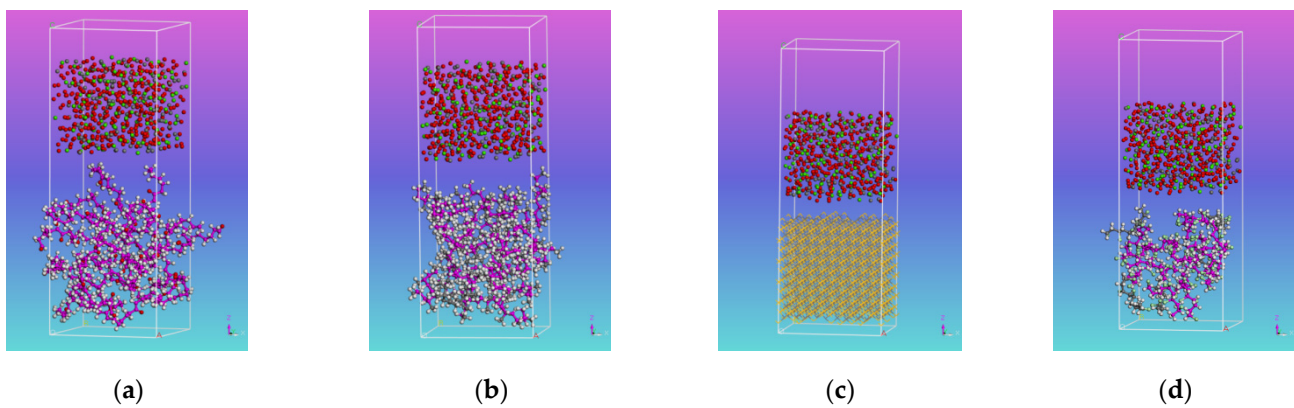


Figure 7. Combination model of the materials and the supercells of (1 0 4) crystal surface. (a) PA6-(1 0 4); (b) PP-(1 0 4); (c) SiC-(1 0 4); (d) PVC-(1 0 4).

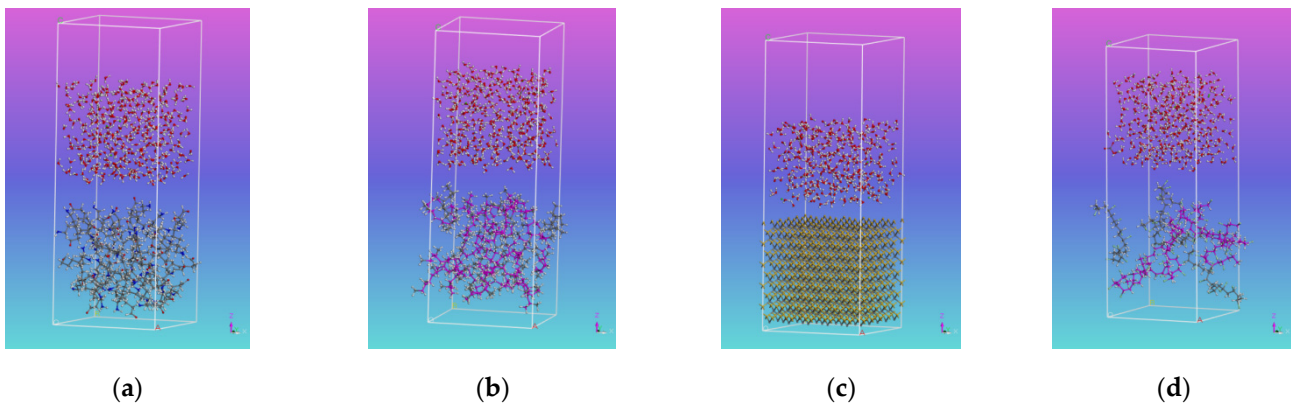


Figure 8. Combination model of the materials and the calcium carbonate aqueous solution. (a) PA6-solution; (b) PP-solution; (c) SiC-solution; (d) PVC-solution.

2.3. Parameter Setting

The MD simulation was performed by the Forcite module in Materials Studio. First, the positions were assigned, and all atomic coordinates of the material layer were fixed through the universal COMPASS force field of high precision. The NVT was adopted because the system pressure was not a key factor. The 100 ps MD simulation under the NVT and velocity scale was first conducted to allow the system to reach an equilibrium state. Then, the MD simulation was performed under the NVT and Andersen thermostatic heat bath, with a time step of 1 fs, a simulation time of 200 ps, the system track being recorded every 1000 steps, a simulation temperature of 298 K, and a cutoff radius of 12.5 Å.

3. Results and Discussion

3.1. System Equilibrium

The equilibrium of the system was determined by the temperature and energy. The accuracy of the simulation was characterized by the ratio of energy convergence parameter ($\Delta E_{converge}$), the total energy fluctuation value rms (E_t), and the kinetic energy fluctuation value rms (E_k), as shown in Formulas (1) and (2) where $E(0)$ and the $E(i)$ were the initial total energy and the total energy when the iteration reached the i th step respectively, and N_{nm} was the times of simulation. When $\Delta E_{converge} \leq 0.001$, $R \leq 0.001$, the calculation results were reliable. After calculation, the $\Delta E_{converge}$ and R of the simulation system at

each temperature conformed to the above value range, indicating that the system reached equilibrium and the simulated calculation results were reliable.

$$\Delta E_{coverge} = \frac{1}{N_{nm}} \sum_i \left| \frac{E(0) - E(i)}{E(0)} \right| \quad (1)$$

$$R = \frac{rms(E_t)}{rms(E_k)} \quad (2)$$

Figure 9 shows the energy output curve of the equilibrium process, and Figure 10 shows the temperature output curve of the equilibrium process. From Figure 9, we can see that the potential energy, kinetic energy, non-bond energy and total energy flattened over time, indicating that the various energy of the system reached the equilibrium. From Figure 10, we can see that the temperature fluctuated 10% around 298 K, indicating that the temperature of the system also reached the equilibrium.

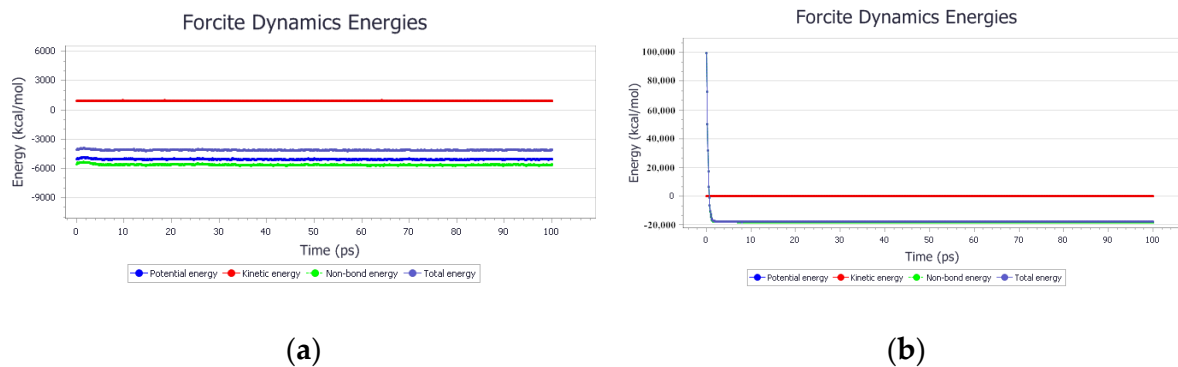


Figure 9. Energy output curve of the system after MD simulation at T = 298 K. (a) The “solid-liquid” model; (b) The “solid-solid” model.

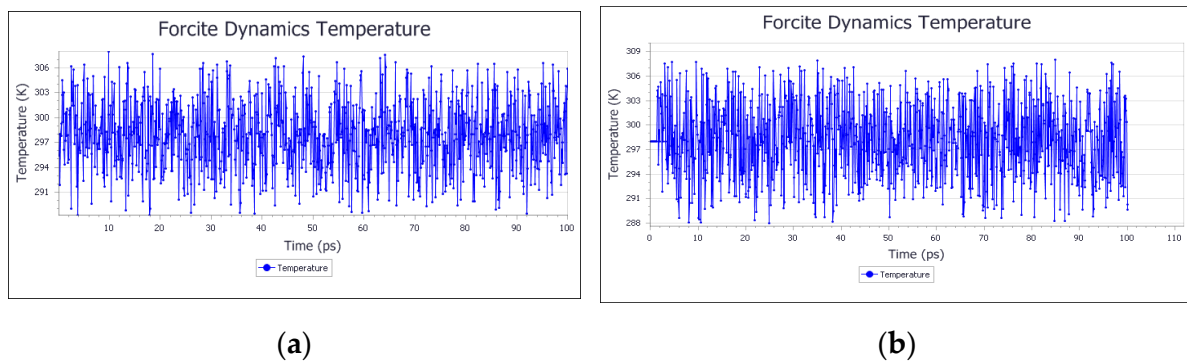


Figure 10. Temperature output curve of the system after MD simulation at T = 298 K. (a) The “solid-liquid” model; (b) The “solid-solid” model.

3.2. Binding Energy Analysis

Interaction between the materials and the crystallized ion solution (two typical growth crystal surfaces of calcium carbonate) was simulated by the molecular dynamics software. If the interaction was very strong, the crystallized ion aqueous solution (two typical growth crystal surfaces of calcium carbonate) would easily attach to the material layer, which meant that the contact area between the pipe wall and the fluffy material was prone to crystallization.

When using the double-layer model for simulation, the data of the fully balanced double-layer structure was collected at an appropriate temperature and a proper ensemble to obtain a series of equilibrium configurations. Then each possible equilibrium configura-

tion was treated as follows: (1) Restore the lower fixed atoms to allow them to move freely, copy three backups, and calculate the total energy (E_{total}) of the system with backup 1; (2) Keep the lower layer of the backup 2 only, delete the upper layer, and calculate the energy (E_{lower}) of the lower layer; (3) Keep the upper layer of the backup 3 only, delete the lower layer, calculate the energy (E_{upper}) of the upper layer, and finally calculate the interaction energy by Formula (3). To calculate the adsorption energy of each material layer, let the interaction energy of the system be ΔE , and the binding energy ($E_{binding}$) be the opposite number of the interaction energy ΔE (Formula (4)). The details are as follows:

$$\Delta E = E_{total} - (E_{upper} + E_{lower}) \quad (3)$$

$$E_{binding} = -\Delta E \quad (4)$$

where E_{total} was the total energy of the system, E_{lower} was the single-point energy of the material layer, E_{upper} was the single-point energy of the crystallized ion aqueous solution system (two typical growth crystal surfaces of calcium carbonate) after interaction. Through simulation calculation, the energy value of the system after the interaction between the "solid + solid" model and the "solid + liquid" model is shown in Table 2, and the changing trend of the binding energy with the materials is shown in Figures 11 and 12.

Table 2. Energy value of the system after interaction between the "solid-solid" model and the "solid-liquid" model (unit: kcal/mol).

Model System		E_{total}	E_{lower}	E_{upper}	ΔE	$E_{binding}$	
solid-solid	CaCO ₃ -PVC	1 – 1 0	−20,132.466	−574.596	−18,487.159	−1070.711	1070.711
		1 0 4	−38,045.005	−542.662	−36,704.997	−797.346	797.346
	CaCO ₃ -PA6	1 – 1 0	−21,054.710	−937.917	−18,467.027	−1649.766	1649.766
		1 0 4	−38,758.331	−928.115	−36,671.616	−1158.600	1158.600
	CaCO ₃ -PP	1 – 1 0	−17,540.010	676.839	−18,487.308	270.459	−270.459
		1 0 4	−35,527.521	616.249	−36,683.798	540.028	−540.028
	CaCO ₃ -SiC	1 – 1 0	−117,279.169	−107,275.987	−18,473.126	8469.944	−8469.944
		1 0 4	−133,290.641	−107,264.983	−36,691.537	10,665.879	−10,665.879
solid-liquid	Solution-PVC	−4703.853	−577.787	−4028.226	−97.840	97.840	
	Solution-PA6	−3849.500	269.641	−3992.464	−126.677	126.677	
	Solution-PP	−3470.688	625.414	−4043.291	−52.811	52.811	
	Solution-SiC	−111,111.148	−107,276.559	−3757.73	−76.859	76.859	

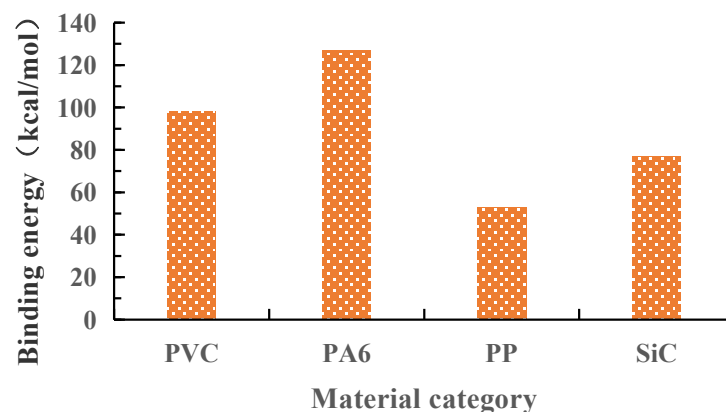


Figure 11. The "solid-liquid" binding energy.

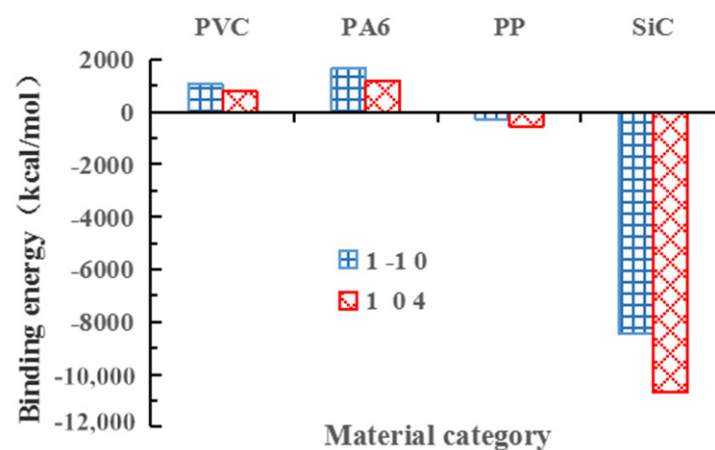


Figure 12. The “solid-and solid” binding energy.

The interaction energy was negative, suggesting that the adsorption of the crystallized ion aqueous solution (two typical growth crystal surfaces of calcium carbonate) on each material surface was a spontaneous process, and a relatively stable system could be formed [20]. As it can be seen from Table 2 and Figure 8, the interaction energy between the four materials and the calcium carbonate aqueous solution was all negative in the “solid + liquid” model, and the binding energy was all positive, indicating that all the four materials had an adsorption effect on the calcium carbonate aqueous solution, and the PA6 had the greatest adsorption effect while the PP had the smallest adsorption effect, with the former being about 2.5 times of the latter. As it can be seen from Table 2 and Figure 9, the interaction energy between the materials of PVC or PA6 and the two typical growth crystals of calcium carbonate was all negative, and the binding energy was all positive, indicating that there was spontaneous adsorption between PVC or PA6 and the two typical growth crystals of calcium carbonate, and the binding energy between either of the two materials and (1 -1 0) crystal surface was greater than that between (1 0 4) crystal surface; the interaction energy between the materials of PP or SiC and the two typical growth crystals of calcium carbonate was all positive, and the binding energy was all negative, indicating that the adsorption between the PP or SiC and the two typical growth crystals of calcium carbonate was impossible unless there was external energy, and the adsorption of (1 0 4) crystal surface was greater than that of (1 -1 0) crystal surface.

Through the above analysis, given the binding energy between the four materials and the crystallized ion aqueous solution, we can select the PP with low binding energy as the materials for drainage pipes; given the binding energy between the four materials and the two typical growth crystals of calcium carbonate, we can select the PP and SiC as the materials for drainage pipes. From the analysis of MD simulation results, we speculated that SiC had the best anti-crystallization effect in drainage pipe flocking, however, the result of the actual indoor macroscopic test [15] was contrary. Thus, the geometric property of the fluffy material (Figure 3) played a major role in the anti-crystallization effect of drainage pipes flocking. Therefore, for better anti-crystallization effect, the PP and SiC can be used as the materials for flocking drainage pipes, but the fluffy material shall have a good geometrical property (smooth surface and straight in the lengthwise direction) so as to maximize the anti-crystallization effect of the drainage pipe flocking.

4. Conclusions

In this paper, the binding energies of PA6, PVC, SiC, PP and calcium carbonate aqueous solution and calcium carbonate were studied by molecular dynamics numerical simulation method.

- (1) PA6, PVC, SiC and PP all have adsorption effect on calcium carbonate solution, and the order of binding energy is PA6 > PVC > SiC > PP.

- (2) The results show that PVC, PA6 and CaCO₃ can spontaneously adsorb on each other, while PP and SiC can only adsorb on each other with the help of external energy. The energy absorbed by (1 0 4) crystal face is greater than that absorbed by (1 -1 0) crystal face.
- (3) The follow-up research can start from the energy of the solution system and the crystal itself and find the technology to make the energy of the system or crystal in a low state, so that the crystal and the pipe are not combined.
- (4) From the point of view of anti-crystallization effect, while considering the binding energy between materials, it is also necessary to ensure the excellent geometric characteristics of pipe (smooth surface and straight length direction), so as to maximize the anti-crystallization effect of flocking drainage pipe. In addition to the binding energy, the molecular weight and production process of polymer should also be considered in the follow-up study.

Author Contributions: Conceptualization, S.L.; Data curation, X.Z., Y.Z. and F.G.; Formal analysis, Y.Z. and F.G.; Writing—original draft, S.L. and X.Z.; Writing—review & editing, S.L. All authors have read and agreed to the published version of the manuscript.

Funding: This research was funded by the National Natural Science Foundation of China (Grant No.51778095), Scientific Research Project of Emei Hanyuan Expressway Project (Grant No. LH-HT-45).

Institutional Review Board Statement: Not applicable.

Informed Consent Statement: Not applicable.

Data Availability Statement: The study did not report any data.

Conflicts of Interest: The authors declare no conflict of interest.

References

1. Jiang, Y.; Du, K.; Tao, L.; Zhao, J.; Xiao, H. Investigation and discussion on blocking mechanism of drainage system in karst tunnels. *Railw. Stand. Des.* **2019**, *63*, 131–135.
2. Tian, C.; Ye, F.; Song, G.; Wang, Q.; Zhao, M.; He, B.; Wang, J.; Han, X. On Mechanism of crystal blockage of tunnel drainage system and preventive countermeasures. *Mod. Tunn. Technol.* **2020**, *57*, 66–76.
3. Xiang, K.; Zhou, J.; Zhang, X.; Huang, C.; Song, L.; Liu, S. Experimental study on crystallization rule of tunnel drainpipe in alkaline environment. *Tunn. Constr.* **2019**, *39*, 207–212.
4. Ye, F.; Tian, C.; Zhao, M.; He, B.; Wang, J.; Han, X. The disease of scaling and clogging in the drainage pipes of a tunnel under construction in yunnan. *China Civ. Eng. J.* **2020**, *53*, 336–341.
5. Zhou, Y.; Zhang, X.; Wei, L.; Liu, S.; Zhang, B.; Zhou, C. Experimental study on prevention of calcium carbonate crystallizing in drainage pipe of tunnel engineering. *Adv. Civ. Eng.* **2018**, *2018*, 1–11. [[CrossRef](#)]
6. Jiang, Y.; Du, K.; Liao, J.; Chen, X.; Xiao, H. Experimental research on maintainability of drainage facilities in lining construction joints of karst tunnel. *Railw. Stand. Des.* **2019**, *63*, 91–96.
7. Su, Y.; Yang, H.; Shi, W.; Guo, H.; Zhao, Y.; Wang, D. Crystallization and morphological control of calcium carbonate by functionalized triblock copolymers. *Colloids Surf. Physicochem. Eng. Asp.* **2009**, *355*, 158–162. [[CrossRef](#)]
8. Kirboga, S.; Oner, M.; Akyol, E. The effect of ultrasonication on calcium carbonate crystallization in the presence of biopolymer. *J. Cryst. Growth* **2014**, *401*, 266–270. [[CrossRef](#)]
9. Su, M.; Han, J.; Li, Y.; Chen, J.; Zhao, Y.; Chadwick, K. Ultrasonic crystallization of calcium carbonate in presence of seawater Ions. *Desalination* **2015**, *369*, 85–90. [[CrossRef](#)]
10. Menzri, R.; Ghizellaoui, S.; Tlili, M. Calcium carbonate inhibition by green inhibitors: Thiamine and pyridoxine. *Desalination* **2017**, *404*, 147–154. [[CrossRef](#)]
11. Hong, Y.; Qian, X.; Li, J.; Yang, H.; Zhang, P. On scavenging performances of cleaning solvents for the clogging in the drainage system of karst tunnels. *Mod. Tunn. Technol.* **2020**, *57*, 160–170.
12. Liu, S.; Zhang, X.; Lü, H.; Liu, Q.; Wang, B. The effect of flocking PVC pipe on the prevention and crystallization of tunnel drains. *Sci. Technol. Eng.* **2018**, *18*, 313–319.
13. Liu, S.; Zhang, X.; Lü, H.; Liu, Q.; Wang, B. The effect of anti-crystallization of tunnel plumage drain pipe under different water filling state. *Sci. Technol. Eng.* **2018**, *18*, 156–163.
14. Liu, S.; Gao, F.; Zhou, Y.; Liu, Q.; Lü, H.; Wang, B.; Xiang, K.; Xiao, D. Effect of fuzz length on the prevention of crystallization of tunnel flocking drainpipes. *Sci. Technol. Eng.* **2019**, *19*, 234–239.
15. Liu, S.; Gao, F.; Zhang, X.; Han, F.; Zhou, Y.; Xiang, K.; Xiao, D. Experimental study on anti-crystallization law of tunnel transverse flocking drainpipe at different velocities. *Asia-Pac. J. Chem. Eng.* **2020**, *15*, 1–9. [[CrossRef](#)]

16. Liu, S.; Zhang, X.; Gao, F.; Wei, L.; Liu, Q.; Lü, H.; Wang, B. Two-dimensional flow field distribution characteristics of flocking drainage pipes in tunnel. *Open Phys.* **2020**, *18*, 139–148. [[CrossRef](#)]
17. Leeuw, N.H.D. Molecular dynamics simulation of the growth inhibiting effect of Fe^{2+} , Mg^{2+} , Cd^{2+} , and Sr^{2+} on calcite crystal growth. *J. Phys. Chem. B* **2002**, *106*, 5241–5249. [[CrossRef](#)]
18. Wang, D.; Huang, L.; Wei, M.; Wang, T.; Tian, Y. MD simulation of influence of high voltage static electric field on crystallization of calcium carbonate. *Ind. Water Wastewater* **2010**, *41*, 76–79.
19. Hädicke, E.; Rieger, J.; Rau, I.U.; Boeckh, D. Molecular dynamics simulations of the incrustation inhibition by polymeric additives. *Phys. Chem. Chem. Phys.* **1999**, *1*, 3891–3898. [[CrossRef](#)]
20. Zhao, W.; Zhang, Q.; Chen, T.; Zhang, J.; Lu, T.; Zhang, H. Molecular dynamics simulation of adsorption of polyelectrolyte on the polystyrene microspheres. *J. Mater. Sci. Eng.* **2009**, *27*, 329–331.